Appl Biochem Biotechnol (2007) 143:101–114
DOI 10.1007/s12010-007-8007-0

Inhibition Kinetics of Cabbage Butterfly (*Pieris rapae* L.) Larvae Phenoloxidase Activity by 3-Hydroxy-4-Methoxybenzaldehyde Thiosemicarbazone

Chao-Bin Xue · Wan-Chun Luo · Lin Jiang · Xian-Ye Xie · Ting Xiao · Lei Yan

Published online: 6 September 2007

Abstract Phenoloxidase (PO) is a key enzyme in insect development, responsible for catalyzing the hydroxylation of tyrosine into *o*-diphenols and the oxidation of *o*-diphenols into *o*-quinones. In the present study, the kinetic assay in air-saturated solutions and the kinetic behavior of PO from *Pieris rapae* (Lepidoptera) larvae in the oxidation of L-tyrosine (a monophenol) and L-DOPA (L-3, 4-dihydroxyphenylalanine) (a diphenol) was studied. The inhibitory effects of 3-hydroxy-4-methoxybenzaldehyde thiosemicarbazone (3-H-4-MBT) on the monophenolase and diphenolase activities of PO were also studied. The results show that 3-H-4-MBT can inhibit both the monophenolase and diphenolase activities of PO. The lag period of L-tyrosine oxidation catalyzed by the enzyme was obviously lengthened and the steady-state activities of the enzyme sharply decreased. The inhibitor was found to be noncompetitively reversible with a K_I (K_I=K_{IS}) of 0.30 μmol/L and an estimated IC_{50} of 0.14±0.02 μmol/L for monophenolase and 0.26±0.04 μmol/L for diphenolase. In the time course of the oxidation of L-DOPA catalyzed by the enzyme in the presence of different concentrations of 3-H-4-MBT, the rate decreased with increasing time until a straight line was approached. The microscopic rate constants for the reaction of 3-H-4-MBT with the enzyme were determined.

Keywords Phenoloxidase · Inhibition kinetics · 3-hydroxy-4-methoxybenzaldehyde thiosemicarbazone · Monophenolase · Diphenolase · *Pieris rapae* (L.)

Abbreviations

V	Initial rate
$[E]_0$	Initial PO concentration
IC_{50}^{D}	The chemical concentration to inhibit 50% of PO activities toward *o*-diphenol

C.-B. Xue · W.-C. Luo (✉) · T. Xiao · L. Yan
College of Plant Protection, Key Laboratory of Pesticide Toxicology and Application Technique, Shandong Agricultural University, Shandong Tai'an 271018, People's Republic of China
e-mail: wcluo@sdau.edu.cn

L. Jiang · X.-Y. Xie
College of Chemistry and Material Science, Shandong Agricultural University, Shandong Tai'an 271018, People's Republic of China

IC_{50}^{M} The chemical concentration to inhibit 50% of PO activities toward monophenol
K_m^D Apparent Michaelis constant of PO toward *o*-diphenol
V_m^D Apparent maximum steady-state rate of PO toward *o*-diphenol

Introduction

Phenoloxidase (PO) (EC 1.14.18.1), also known as tyrosinase, a copper-containing bifunctional enzyme, is highly conserved in microorganisms, animals and plants [1–3]. It is involved in the formation of pigments and is the key enzyme in melanin formation in melanocytes. PO oxidase catalyzes two distinct reactions of melanin synthesis, the hydroxylation of a monophenol (monophenolase activities) and the conversion of an *o*-diphenol to the corresponding *o*-quinone (diphenolase activities) [4]. In insects, PO is uniquely associated with three physiologically important biochemical processes—sclerotization of the insect cuticle, wound healing, and defensive encapsulation—and melanization of foreign organisms [5]. The production of *o*-quinones by PO is the initial step in the biochemical cascade of sclerotization, quinone tanning, and melanin biosynthesis, processes that play several major roles in insect development and immunity.

During the catalysis reaction, PO exists in three states: E_{met} (*met*-PO, with Cu(II)–Cu(II) in the active site), E_{deoxy} (*deoxy*-PO, reduced form of PO with Cu(I)–Cu(I) in the active site), and E_{oxy} (*oxy*-PO, with $\text{Cu(II)} - O_2^{2-} - \text{Cu(II)}$ in the active site) [6–8]. Structural models for the active site of these three forms of PO have been proposed [3, 9–11]. The reactions catalyzed by these three forms of the enzyme are summarized in Scheme 1.

Here *M* and *D* represent two different substrates, monophenol (L-tyrosine) and *o*-diphenol (L-DOPA). *Q* is the product—quinone. E_{oxy}, E_{met} and E_{d} (*deoxy*-PO) represent the three forms of the enzyme. E_{oxy}–*M*, E_{met}–*M*, E_{oxy}–*D*, E_{met}–*D* are enzyme-substrate complexes, whereas k_+ and k_- are rate constants for the forward and reverse reactions of each step. The *oxy*-PO starts the turnover by acting on the monophenol (*M*), which is hydroxylated to the *met*-PO-diphenol intermediate (E_{met}–*D*). At this point, the enzyme can oxidize *D* to *o*-quinone (*Q*), produce the *deoxy*-PO (E_{d}), or release *D* to make the met form (E_{met}), which binds with

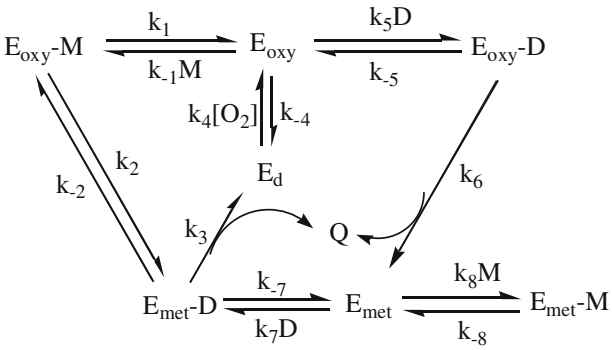

Scheme 1 Forward and reverse reactions catalyzed by three forms of the phenoloxidase (PO) enzyme

M to produce the inactive form, E_{met}–M. If *Q* is quite unstable, as it occurs in the case of *o*-dopaquinone, *D* is recycled to the medium through intramolecular cyclization and further redox steps. This process involves the transformation of the E_{met} form of the enzyme (which is inactive toward *M*) into the E_{oxy} form (which is active toward *M*), giving rise to a characteristic lag period [12–15]. In such cases, the system would reach a steady state.

Recently, the crystallographic evidence that dinuclear copper center of tyrosinase was reported, the copper-bound crystal structures including a metal-free tyrosinase and a "caddie" protein ORF378, which can assist transport of two Cu(II) ions into tyrosinase catalytic center. The structure suggested that the caddie protein covers the hydrophobic molecular surface of tyrosinase and interferes with the binding of a substrate tyrosine to the catalytic site of tyrosinase. Furthermore, the E_{met} form of Cu(II)-bound tyrosinase complexed with ORF378 and that of its E_{deoxy} and E_{oxy} forms by soaking the E_{met} form crystal in a solution containing NH_2OH and H_2O_2, respectively, were also reported. The crystallographic investigation showed evidence that the tyrosinase active center formed by dinuclear coppers is flexible during the catalysis [3].

Naturally, the two copper atoms in the active site of PO have become the targets of inhibition studies, and PO inhibitors have increasingly been used in medicinal and cosmetic products [16, 17]. Some copper chelators were found to inhibit mushroom tyrosinase; other inhibitors of mushroom tyrosinase include flavor compounds from olive oil and flavonol compounds from the saffron flower [18, 19].

As PO is one of the key enzymes in the insect molting process [20], screening one of these inhibitors might ultimately provide clues for the development of insect control [21–23]. To our knowledge, the inhibition kinetics of mushroom tyrosinase activity by some compounds has been reported, such as hexylresorcinol, dodecylresorcinol [24], 3,5-dihydroxyphenyl decanoate [25], *p*-alkoxybenzoic acids [26], and 3,5-dihydroxystilbene [27]. In the present study, the chemical 3-hydroxy-4-methoxybenzaldehyde thiosemicarbazone (3-H-4-MBT) has a thiosemicarbazone structure, which is a potent copper chelate structure. Accordingly, the inhibitory effects on PO from *P. rapae* larvae were studied, the inhibition kinetics of 3-H-4-MBT on monophenolase and diphenolase activities of PO were investigated in detail, and inhibitory mechanism was also discussed with an action model.

Materials and Methods

Insects and Reagents

Pieris rapae larvae were reared on Chinese cabbage *Brassica parachinesi* (Bailey) in a greenhouse at 25±1°C with a 14:10 h light/dark photoperiod. The fifth instar larvae were gathered for the experiments. L-DOPA (L-3, 4-dihydroxyphenylalanine), L-tyrosine, and dimethyl sulfoxide (DMSO) were purchased from Aldrich Chemical Co. (Milwaukee, WI, USA). 3-hydroxy-4-methoxybenzaldehyde thiosemicarbazone (3-H-4-MBT) studied in this work was designed and synthesized in our laboratory, it was purified by chromatography over silica gel, and its chemical structure was confirmed by ^{1}H NMR spectra and mass spectroscopy as well as elemental analyses [28]. Sephadex G-100 was purchased from Amersham Pharmacia Biotech (Uppsala, Sweden). All other reagents were local products of analytical grade. The water was redistilled and ion-free.

Enzyme Purification

All procedures were carried out at 4°C. The fifth instar *P. rapae* larvae were homogenized in a fivefold weight of ice-cold 0.2 mol/L sodium phosphate buffer (pH 6.9), and then the homogenate was placed steadily in 4°C for 2 h, and centrifuged at 9,310×*g* for 30 min. The supernatant under the fat layer was collected as the crude enzyme extract, and was brought to 35% saturation with solid ammonium sulfate. The precipitate was collected by centrifugation at 9310×*g* for 30 min and then redissolved in a minimum volume of the same phosphate buffer, and was dialyzed against the 0.01 mol/L sodium phosphate buffer (pH 6.9). The dialyzed solution was loaded onto a Sephadex G-100 column (2.5×60 cm), which was equilibrated with 0.01 mol/L sodium phosphate buffer (pH 6.9), and fractions having high activities were collected. The gel filtration chromatography process increased the specific activities up to 6.22-fold that of the crude enzyme extract.

Enzyme Assays

PO catalyzes the reaction between two substrates, a phenolic compound and oxygen. All assays were carried out in air-saturated solutions. Enzymatic activities assayed by monitoring dopachrome formation at 475 nm (ε=3,700 [mol^{-1} L cm^{-1}]) [29] accompanying the oxidation of the substrate (L-tyrosine or L-DOPA). The assay was performed as previously described [30], with slight modifications. The reaction media (2 ml) for PO activities contained 1 mmol/L L-DOPA or 4 mmol/L L-tyrosine in 0.1 mol/L Na_2HPO_4–NaH_2PO_4 buffer (pH 6.9), the indicated concentration of 3-H-4-MBT and 3.3% DMSO. In this method, different amounts of 3-H-4-MBT were dissolved in DMSO solution and added to the test tube. To this mixture was added 1.9 mL of substrate solution in Na_2HPO_4–NaH_2PO_4 buffer (pre-warmed to 37°C) and 0.1 mL of aqueous enzyme solution. This final solution was immediately monitored for 100 s for the formation of dopachrome by measuring the linear increase in optical density at 475 nm at a constant temperature of 37°C. Absorption was recorded using a Hitachi UV-2201 spectrophotometer. The extent of inhibition was expressed as the chemical concentration to inhibit 50% of the enzyme activities (IC_{50}). The kinetic and inhibition constants were obtained by the previously described method [15, 30].

Results

The Kinetics of PO for the Oxidation of L-tyrosine and L-DOPA

The kinetic behavior of PO was studied during the oxidation of different concentrations of L-DOPA and L-tyrosine, and progress curves were determined for the enzyme at each concentration. When the diphenolase activities of PO was assayed using L-DOPA as the substrate, the reaction immediately reached a steady-state rate (Fig. 1, curves 1–4). It is shown as a straight line that passes through the original point of the coordinate with a slope equal to the initial rate (v_0). The relationship of the initial rate and the concentration of substrate (L-DOPA) followed Michaelis–Menten kinetics. Kinetic parameters for the diphenolase activities of PO are shown in Fig. 5 (line 0) as a Lineweaver–Burk plot. The apparent Michaelis constant K_m^D is 1.35±0.06 mmol/L and the apparent maximum velocity $\left(V_m^D\right)$ is 1.81±0.04 mmol/L/min. When the monophenolase activities of PO was assayed using L-tyrosine as the substrate, a remarkable lag period, characteristic of monophenolase

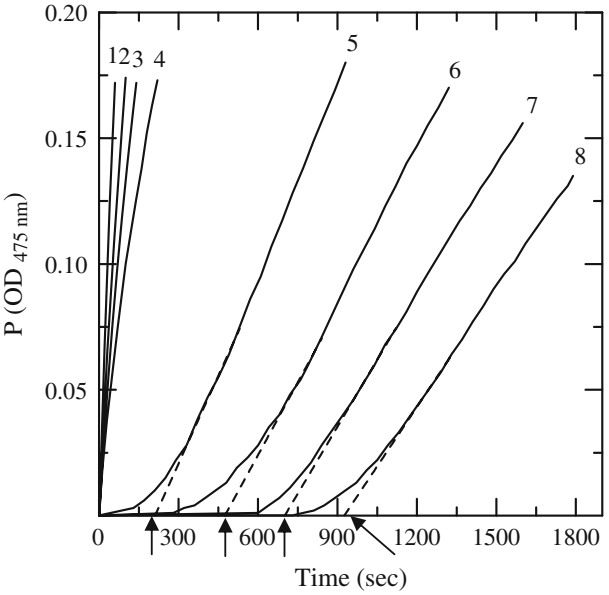

Fig. 1 Progress curves for the inhibition for PO from *P. rapae* larvae by 3-H-4-MBT. Curves 1–4 show the effects of the inhibitor on the *o*-diphenolase activity of the enzyme. The reaction media contained L-DOPA 0.5 mmol/L in 0.1 mol/L Na_2HPO_4–NaH_2PO_4 buffer pH 6.9. Curves 5–8 show the effects of 3-H-4-MBT on the monophenolase activity of the enzyme. L-tyrosine (4 mmol/L) as the substrate. 3-H-4-MBT concentration were (1) and (5) 0 μmol/L, (6) 0.05 μmol/L, (2) and (7) 0.1 μmol/L, (8) 0.15 μmol/L, (3) 0.2 μmol/L, (4) 0.4 μmol/L. The arrows show the lag period

activities, was observed with the simultaneous appearance of the first stable product, dopachrome (Fig. 1, curves 5–8). The system reached a constant rate after the lag period, which was estimated by extrapolation of the linear portion of the product accumulation curve to the abscissa [31]. After the reaction system reached a steady state, the curve of product increased linearly with increasing reaction time.

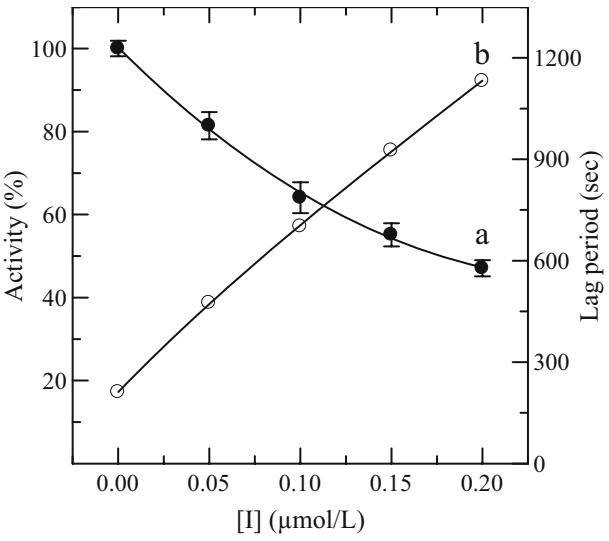

Fig. 2 Effect of 3-H-4-MBT on the steady-state rate of monophenolase activity (a) and the lag period of PO (b) for the oxidation of L-tyrosine. Assay conditions were as described for Fig. 1, L-tyrosine (4 mmol/L) as substrate

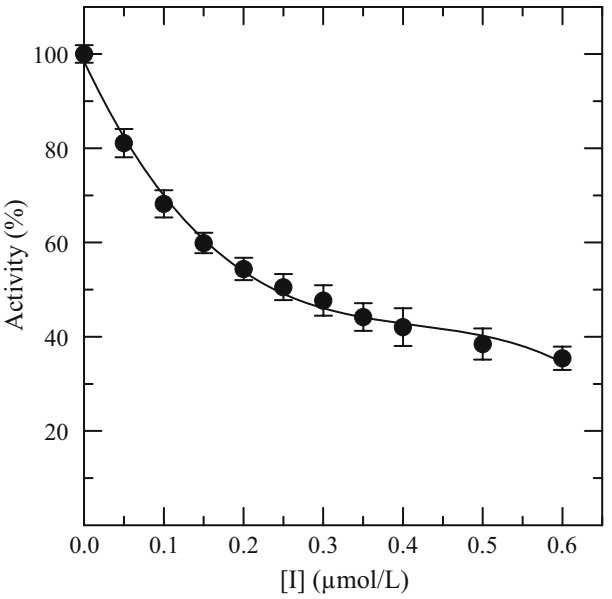

Fig. 3 The inhibition of 3-H-4-MBT on the activity of PO from *P. rapae* larvae for the catalysis of L-DOPA at 37°C. Assay conditions: 2 ml 0.1 mol/L Na_2HPO_4–NaH_2PO_4 buffer pH 6.9, containing 1 mmol/L L-DOPA

The Effect of 3-H-4-MBT on the Monophenolase Activities of PO

The effect of 3-H-4-MBT on the monophenolase activities of PO was tested using L-tyrosine as the substrate. Figure 2 shows that 3-H-4-MBT inhibited monophenolase activities at the steady-state rate (curve *a*) and lengthened the lag period of PO (curve *b*). The results indicate that the length of the lag period increased with greater concentrations of 3-H-4-MBT, and that the steady-state rates, which were the slopes of the linear portions of the kinetic curves, decreased accordingly; 0.2 μmol/L of 3-H-4-MBT resulted in an extension of the lag period from 210.86 to 1131.35 s. The IC_{50} value was estimated as 0.14±0.02 μmol/L.

Table 1 Kinetics parameters and microscopic inhibition rate constants of phenoloxidase from *P. rapae* larvae by 3-H-4-MBT.

Parameter	Rate/Inhibition
IC_{50}^{D}	0.26±0.04 μmol/L
IC_{50}^{M}	0.14±0.02 μmol/L
K_m^D	1.35±0.06 mmol/L
V_m^D	1.81±0.04 mmol/L/min
Inhibition	Reversible
Inhibition type	Noncompetitive
K_I	0.30 μmol/L
K_{IS}	0.30 μmol/L
k_{+0}	1.79×10^{-2} s^{-1}
k_{-0}	2.69×10^{-6} s^{-1}

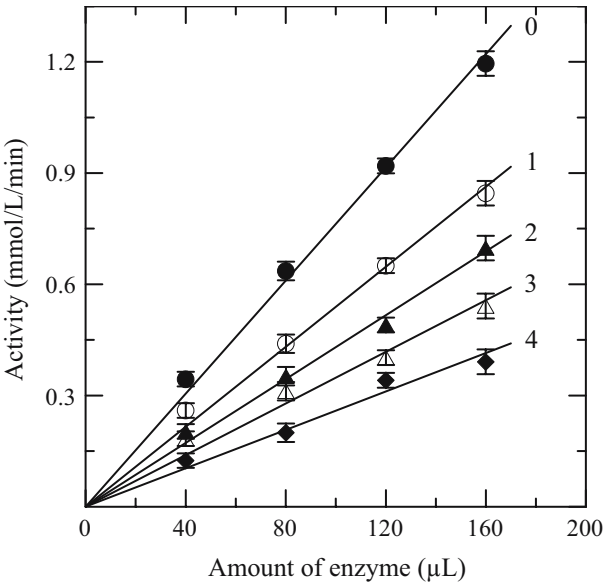

Fig. 4 The effects of concentrations of 3-H-4-MBT on the activity of PO from *P. rapae* larvae for the catalysis of L-DOPA at 37°C. Assay conditions were as described for Fig. 3 except for change the concentrations of enzyme. Concentrations of 3-H-4-MBT for curves 0–4 were 0, 0.1, 0.2, 0.3, and 0.4 μmol/L, respectively

The Effect of 3-H-4-MBT on the Diphenolase Activities of PO

The effect of 3-H-4-MBT on the diphenolase activities of PO was examined by measuring the oxidation of L-DOPA. The results showing the kinetics of product generation at different concentrations of inhibitor were represented as straight lines that passed through the original points. The slopes of the lines decreased with increasing 3-H-4-MBT concentrations (Fig. 1 curves 1–4), indicating that the inhibition of diphenolase activities was dependent on the concentration of 3-H-4-MBT, as shown in Fig. 3. As the concentrations of 3-H-4-MBT increased, the remaining enzymatic activities of PO rapidly decreased. The IC_{50} value was estimated as 0.26±0.04 μmol/L and is summarized in Table 1.

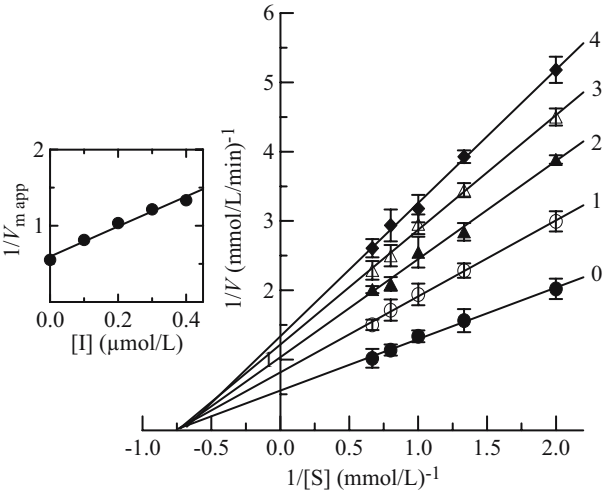

Fig. 5 Lineweaver-Burk plots for inhibition of 3-H-4-MBT on the activity of PO from *P. rapae* larvae for the catalysis of L-DOPA at 37°C, pH 6.9. Assay conditions were as described for Fig. 3 except for change in the substrate concentrations. Concentrations of 3-H-4-MBT for curves 0–4 were 0, 0.1, 0.2, 0.3, and 0.4 μmol/L, respectively. The inset represents the plot of $1/V_{m\ app}$ versus the 3-H-4-MBT concentration for determining the inhibition constants K_I

Inhibition of PO Diphenolase Activities by 3-H-4-MBT was Reversible and Noncompetitive

The relationship between diphenolase activities and enzyme concentration in the presence of different concentrations of inhibitor was studied (Fig. 4). The plots of enzyme activities versus enzyme concentration at different inhibitor concentrations yielded straight lines passing through the origin. Higher inhibitor concentrations were associated with decreasing slopes, demonstrating that the inhibition of PO by 3-H-4-MBT was reversible. The presence of 3-H-4-MBT did not reduce the amount of the enzyme, but rather, resulted in the inhibition of activities of the enzyme involved in the oxidation of L-DOPA.

The kinetic behavior of PO during the oxidation of L-DOPA was also determined. Under the conditions employed in this investigation, the oxidation of L-DOPA by PO followed Michaelis–Menten kinetics. This result, shown in Fig. 5, revealed that 3-H-4-MBT was a noncompetitive inhibitor, as increases in 3-H-4-MBT concentrations resulted in a family of lines with a common intercept on the 1/[S] axis but with different slopes. The apparent value of V_m was decreased with no effect on K_m. The observed behavior showed that the inhibitor can combine with both the free enzyme (E) and the enzyme–substrate (ES) complex, and that the equilibrium constants for inhibitor binding with free enzyme, K_I, and the enzyme–substrate complex, K_{IS}, were the same. The inhibition constant can be obtained from a plot of the vertical intercept ($1/V_{m\ app}$) versus the inhibitor concentration, as shown in the Fig. 5 inset. The obtained inhibition constant ($K_I=K_{IS}$) was 0.30 μmol/L.

Determination of 3-H-4-MBT Microscopic Rate Constants

The progress-of-substrate-reaction method previously described by Tsou [32] was used to study the inhibitory kinetics for PO from *P. rapae* by 3-H-4-MBT. In this method, 0.1 mL of the aqueous solution of PO was added to 2.0 mL of an assay system containing 1 mmol/L L-DOPA in 0.1 mol/L Na_2HPO_4–NaH_2PO_4 buffer (pH 6.9) containing different concentrations of 3-H-4-MBT. The substrate reaction progress curve was analyzed to obtain the reaction rate constants. The reaction was carried out at a constant temperature of 37°C.

For slow, reversible inhibition with fractional residue activity, the kinetic model of the enzyme reacting with the substrate and the inhibitor can be written as:

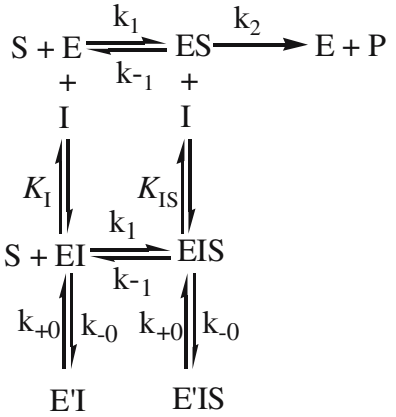

where E, S, I and P denote enzyme, substrate, inhibitor (3-H-4-MBT) and product, respectively. EI, ES and EIS are the respective complexes. E'I and E'IS are inactive enzyme

forms. K_I and K_{IS} are the inhibition constants for the inhibitor (3-H-4-MBT), k_{+0} and k_{-0} are rate constants for forward and reverse inactivation of the enzyme, respectively.

Assuming that $[S] \gg [E_0]$, $[I] \gg [E_0]$ and that the modification reactions are relatively slow compared with the setup of the steady state of the enzymatic reaction:

$$[E] = \frac{K_I \cdot K_m}{(K_I + [I])(K_m + [S])} \cdot [E_T] \tag{1}$$

$$[\mathrm{ES}] = \frac{K_I \cdot [S]}{(K_I + [I])(K_m + [S])} \cdot [E_T]$$

$$[\mathrm{EI}] = \frac{K_I \cdot [I]}{(K_I + [I])(K_m + [S])} \cdot [E_T]$$

$$[\mathrm{ESI}] = \frac{[I] \cdot [S]}{(K_I + [I])(K_m + [S])} \cdot [E_T]$$

where $[E_T] = [E] + [\mathrm{ES}] + [\mathrm{EI}] + [\mathrm{EIS}]$ and $\left[E_T^*\right] = [E'I] + [E'\mathrm{IS}]$ are the total concentrations of the unmodified and modified enzymes, $[E_0] = [E_T] + \left[E_T^*\right]$, and K_m is the Michaelis constants. The rate of decrease of E_T can be given in the following form:

$$\begin{aligned} -\frac{\mathrm{d}[E_T]}{\mathrm{d}t} &= \frac{\mathrm{d}\left[E_T^*\right]}{\mathrm{d}t} \\ &= k_{+0}\left([\mathrm{EI}] + [\mathrm{ESI}] - k_{-0}\left[E_T^*\right]\right) \\ &= A[E_T] - B[E_0] \end{aligned} \tag{2}$$

where,

$$A = \frac{k_{+0} \cdot [I]}{K_I + [I]} + k_{-0} \quad \text{and} \quad B = k_{-0} \tag{3}$$

A and B are the apparent rate constants for inactivation and reactivation, respectively. The product formation can be written as:

$$[P]_t = \frac{v \cdot k_{-0}}{A} \cdot t + \frac{v \cdot (A - k_{-0})}{A^2} \cdot \left(1 - e^{-A \cdot t}\right) \tag{4}$$

where $[P]_t$ is the product concentration formed at reaction time t. $[S]$ and $[I]$ are the concentrations of the substrate and inhibitor, v is the initial reaction rate in the absence of the inhibitor. When t is sufficiently large, the curves become straight lines and the product concentration is written as $[P]_\mathrm{calc}$:

$$[P]_\mathrm{calc} = \frac{v \cdot k_{-0}}{A} \cdot t + \frac{v \cdot (A - k_{-0})}{A^2} \tag{5}$$

A plot of $[P]_\mathrm{calc}$ vs. t gives a straight line with:

$$slope = \frac{v \cdot k_{-0}}{A} \tag{6}$$

$$[P]_\mathrm{calc} - [P]_t = \frac{v}{A^2}(A - k_{-0}) \cdot e^{-A \cdot t} \tag{7}$$

Combining Eqs. (4) and (5) gives:

$$\ln\left([P]_{\text{calc}} - [P]_t\right) = -A \cdot t + \ln\left[\frac{v \cdot (A - k_{-0})}{A^2}\right] \tag{8}$$

where $[P]_{\text{calc}}$ is the product concentration to be expected from the straight-line portions of the curves as calculated from Eq. (5) and $[P]_t$ is the product concentration actually observed at time t. Plots of $\ln\left([P]_{\text{calc}} - [P]_t\right)$ vs. t give a series of straight lines at different concentrations of inhibitor [3 -4-MBT] with slopes of $-A$. A plot of $[P]_{\text{calc}}$ vs. t gives a straight line with a slope k_{-0}/A, which can be used to determine k_{-0}.

The apparent forward rate constant, A, is independent of the substrate concentration, but depends on the inhibitor concentration [3-H-4-MBT].

Kinetics of the Substrate Reaction in the Presence of Different 3-H-4-MBT Concentrations

The progress-of-substrate-reaction method previously described by Tsou [32] was used to study the inactivation kinetics for PO from *P. rapae* by 3-H-4-MBT. The time course of the oxydation of the substrate in the presence of different 3-H-4-MBT concentrations is shown in Fig. 6a. At each 3-H-4-MBT concentration, the rate decreased with increasing time until a straight line was approached. The results show that at a certain 3-H-4-MBT concentration, the inactivation was a reversible reaction with fractional residual activity and the substrate gives very little protection. The form of Eq. (5) suggests that a plot of $[P]_{\text{calc}}$ vs. t will give

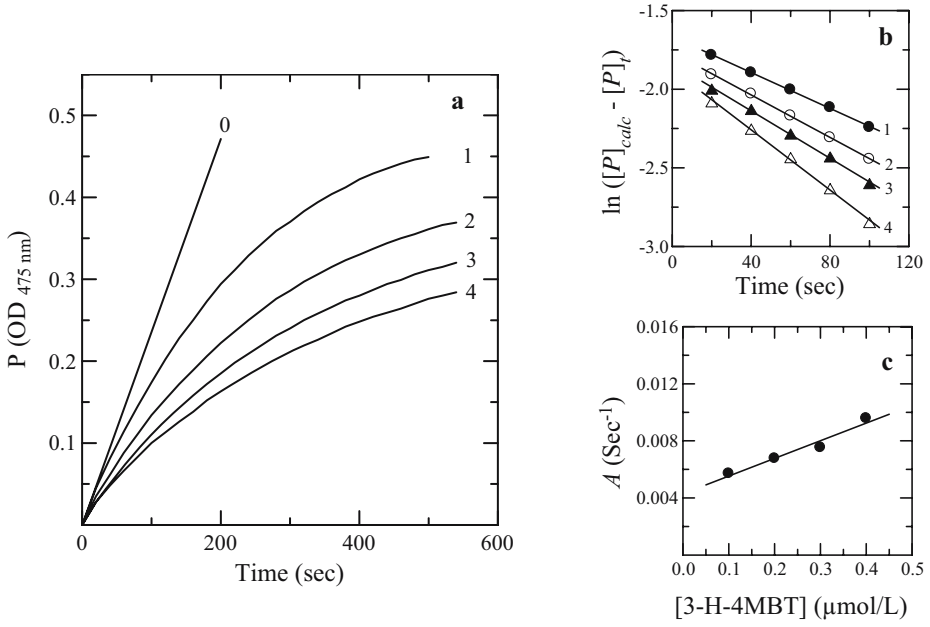

Fig. 6 Course of the substrate reaction in the presence of different concentrations of 3-H-4-MBT. Assay conditions were as described for Fig. 4a. The time course of the substrate oxidation reaction. The concentrations of 3-H-4-MBT for curves 0–4 were 0, 0.1, 0.2, 0.3, and 0.4 µmol/L, respectively. (b) Plots of $\ln([P]_{\text{calc}}-[P]_t)$ vs time. Data were taken from curves 1–4 in (a). (c) The apparent forward inactivation rate constants for various 3-H-4-MBT concentrations, the data were taken from curves 1–4 in (b)

a series of straight lines with slopes of ($v \cdot k_{-0}/A$) at different 3-H-4-MBT concentrations. From Eq. (8), plots of $\ln\left([P]_{calc} - [P]_t\right)$ vs. t give a series of straight lines at different 3-H-4-MBT concentrations with slopes of $-A$, the apparent forward rate constant, Fig. 6b. Figure 6c shows the dependence of A on the 3-H-4-MBT concentration. The initial rate (v) of reaction in the presence of 3-H-4-MBT and the microscopic rate constant of the reverse inactivation of the enzyme (k_{-0}) for these experimental conditions are listed in Table 1.

Kinetics of the Reaction at Different Substrate Concentrations in the Presence of 3-H-4-MBT

Figure 7a shows the kinetic courses of the reaction at different L-DOPA concentrations in the presence of 3-H-4-MBT (0.2 μmol/L). Similarly, plots of $\ln\left([P]_{calc} - [P]_t\right)$ vs. t give a family of straight lines at different substrate concentrations with slopes of $-A$, Fig. 7b. The apparent forward rate constants, A, can be obtained through suitable plots. A plot of the slopes of the straight lines in Fig. 7b vs. L-DOPA concentration [S] gives a horizontal straight line, Fig. 7c, indicating that the substrate concentration [S] does not affect the microscopic rate constants k_{+0} and k_{-0}.

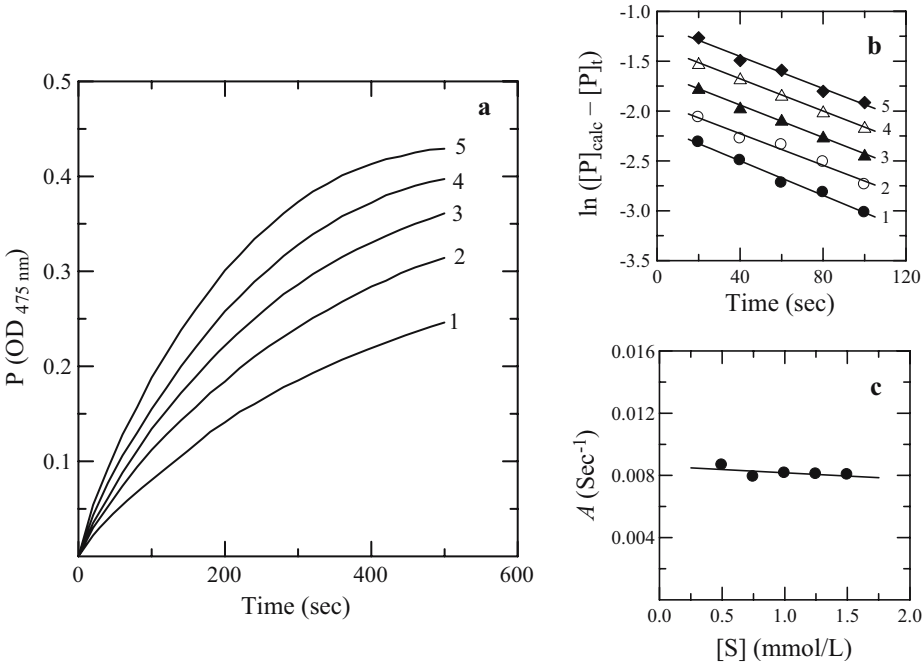

Fig. 7 Course of the substrate reaction at different substrate concentration in the presence of 3-H-4-MBT. Experimental conditions were the same as those for Fig. 6 except the L-DOPA concentrations were different. (a) The time course of the substrate oxidation reaction. The concentrations of L-DOPA for curves 1–5 were 0.5, 0.75, 1.0, 1.25, and 1.5 mmol/L, respectively. (b) Plots of $\ln([P]_{calc}-[P]_t)$ vs time. Data were taken from curves 1–5 in (a). (c) The apparent forward inactivation rate constants (A) vs. L-DOPA concentrations in the presence of 3-H-4-MBT

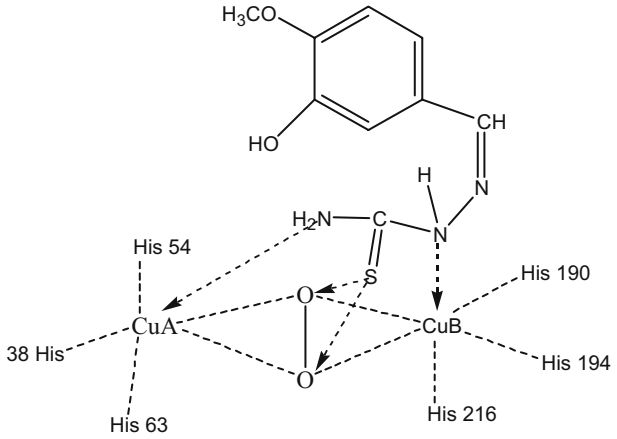

Fig. 8 Interaction model of 3-H-4-MBT against PO active site

Discussion

PO has both monophenolase and diphenolase activities. During catalysis, PO exists in three forms: E_{met}, E_{deoxy}, and E_{oxy}. E_{oxy} has monophenolase activities, both E_{met} and E_{deoxy} have diphenolase activities, and E_{deoxy} can combine with oxygen [11]. The E_{met} form does not act on monophenols but has an affinity for them, binding them to form a deadend complex that may explain the lag period before attainment of the steady-state rate [1]. Here L-tyrosine and L-DOPA were used as substrates for monophenolase and diphenolase activities assays that were carried out in air-saturated solutions. The lag period can be estimated by extrapolation of the linear portion of the product accumulation curve to the *X*-axis. As shown in Fig. 1, the data indicate that the addition of 3-H-4-MBT lengthens the lag period of monophenolase formation, decreases the steady-state rates of both monophenolase and diphenolase activities, and slows the rate of dopachrome formation.

It is well-known that the lag period can be shortened or even abolished by the presence of catalytic amounts of transition metal ions, especially *o*-diphenols such as quercetin [11, 18]. Here, we found that 3-H-4-MBT could inhibit monophenolase activities and extend the lag period. It is likely that the inhibitor combines with the E_{met} and E_{oxy} forms to generate E_{met}–*I* and E_{oxy}–*I* complexes. The inhibition of PO by 3-H-4-MBT was reversible and noncompetitive, indicating that the inhibitor can bind the free enzyme (*E*) to form both the EI and ESI complexes.

Tyrosinase is classified into the type-3 copper protein family, as are catechol oxidase and the respiratory pigment hemocyanin. When the catechol oxidase in a complex with a potent inhibitor, phenylthiourea, in the substrate-binding pocket, the Tyr^{98} ring is aligned perfectly with the aromatic ring of phenylthiourea [3]. Phenylthiourea and 3-H-4-MBT belong to thiourea compounds, which have the thiourea common structure both. In addition, as the size of substrate-binding pocket of phenoloxidase is actually large [3], the inhibitor 3-H-4-MBT may be accommodated into the pocket, and coordination bonds between the atom of nitrogen in 3-H-4-MBT and Cu^{2+} in $Cu(II) - O_2^{2-} - Cu(II)$, and, the thioether bond between the sulfur atom and O^{2-} in $Cu(II) - O_2^{2-} - Cu(II)$ were formed in the active site of phenoloxidase, where the arrows are located in Fig. 8. Besides, some hydrogen bonds were formed by the inhibitor reaction with primary amino group in the active site. Consequently, the enzyme lost its catalysis activities, which may be the possible inhibitory mechanism of 3-H-4-MBT on PO.

PO plays a key role in normal insect development, so it may be potential to control pests by inhibiting or disturbing the enzyme. This may be a useful basis for the development of novel insecticides to replace traditional chemicals, many of which currently pose serious threats to the environment and/ or have been associated with resistance, toxic residues, and/ or resurgence in target pest populations. Here, we show that 3-H-4-MBT is an effective PO inhibitor, and reveal a few of the mechanistic details of the reaction. Hopefully, this work will provide the basis for the design of effective, selective PO inhibitors and the development of novel candidate insecticides.

Acknowledgments The present investigation was supported by grant NO. 30571237 of the Natural Science Foundation of the People's Republic of China for Wan-Chun Luo.

References

1. Sánchez-Ferrer, A., Rodríguez-López, J. N., García-Cánovas, F., & García-Carmona, F. (1995) Tyrosinase: a comprehensive review of its mechanism. *Biochimica et Biophysica Acta, 1247*, 1–11.
2. Chase, M. R., Raina, K., Bruno, J., & Sugumaran, M. (2000) Purification, characterization and molecular cloning of prophenoloxidase from *Sarcophaga bullata*. *Insect Biochemistry and Molecular Biology, 30*, 953–967
3. Matoba, Y., Kumagai, T., Yamamoto, A., Yoshitsu, H., & Sugiyama, M. (2006) Crystallographic evidence that dinuclear copper center of tyrosinase is flexible during catalysis. *Journal of Biological Chemistry, 281*, 8981–8990.
4. Chen, Q. X., Liu, X. D., & Huang, H. (2003) Inactivation kinetics of mushroom tyrosinase in the dimethyl sulfoxide solution. *Biochemistry (Moscow), 68*, 644–649.
5. Ashida, M., & Brey, P. (1995) Role of the integument in insect defense: prophenoloxidase cascade in the cuticular matrix. *Proceedings of the National Academy of Sciences of the United States of America, 92*, 10698–10702.
6. Mason, H. S. (1956) Structure and functions of the phenolase complex. *Nature, 177*, 79–81.
7. Makino, N., McMahill, P., Mason, H. S., & Moss, T. H. (1974) The oxidation state of copper in resting tyrosinase. *Journal of Biological Chemistry, 249*, 6062–6066.
8. Espín, J. C., Varón, R., Fenoll, L. G., Gilabert, M. A., García-Ruíz, P. A., Tudela-Varón, J. R., et al. (2000) Kinetic characterizations of the substrate specificity and mechanism of mushroom tyrosianse. *European Journal of Biochemistry, 267*, 1270–1279.
9. Rodríguez-López, J. N., Tudela-Varón, J. R., García-Carmona, F., & García-Canovas, F. (1992) Analysis of a kinetic model for melanin biosynthesis pathway. *Journal of Biological Chemistry, 267*, 3801–3810.
10. Nakayama, T., Sato, T., Fukui, Y., Yonekura-Sakakibara, K., Hayashi, H., Tanaka, Y., et al. (2001) Specificity analysis and mechanism of aurone synthesis catalyzed by aureusidin synthase, a polyphenol oxidase homolog responsible for flower coloration. *FEBS Letters, 499*, 107–111.
11. Fenoll, L. G., Rodríguez-López, J. N., García-Sevilla, F., García- Ruiz, P. A., Varón, R., García-Cánovas, F., et al. (2001) Analysis and interpretation of the action mechanism of mushroom tyrosinase on monophenols and diphenols generating highly unstable o-quinones. *Biochimica and Biophysica Acta, 1548*, 1–22.
12. Espín, J. C., Jolivt, S., & Wichers, H. J. (1999) Kinetic study of the oxidation of _-L-glutaminyl-4-hydroxybenzene catalyzed by (*Agaricus Bisporus*) tyrosinase. *Journal of Agricultural and Food Chemistry, 47*, 3495–3502.
13. Fenoll, L. G., Rodríguez-López, J. N., García-Sevilla, F., Tudela, J., García- Ruiz, P. A., Varón, R., et al. (2000) Oxidation by mushroom tyrosinase of monophenols generating slightly unstable o-quinones. *European Journal of Biochemistry, 267*, 5865–5878.
14. Rodríguez-López, J. N., Fenoll, L. G., & García-Ruiz, P. A. (2000) Stopped-flow and steady-state study of the diphenolase activity of mushroom tyrosinase. *Biochemistry, 39*, 10497–10506.
15. Xie, L. P., Chen, Q. X., Huang, H., Liu, X. D., Chen, H. T., & Zhang, R. Q. (2003) Inhibitory effects of cupferron on the monophenolase and diphenolase activity of mushroom tyrosinase. *International Journal of Biochemistry and Cellular Biology, 35*, 1658–1666.
16. Maeda, K., & Fukuda, M. (1991) In vitro effectiveness of several whitening cosmetic components in human melanocytes. *Journal of the Society of Cosmetic Chemists, 42*, 361–368.

17. Friedman, M. (1996) Food browning and its prevention: an overview. *Journal of Agricultural and Food Chemistry, 44*, 631–653.
18. Kubo, I., & Kinst-Hori, I. (1999) Flavonols from saffron flower: tyrosinase inhibitory activity an inhibition mechanism. *Journal of Agricultural and Food Chemistry, 47*, 4121–4125.
19. Kubo, I., & Kinst-Hori, I. (1999) Tyrosinase inhibitory activity of the olive oil flavor compounds. *Journal of Agricultural and Food Chemistry, 47*, 4574–4578.
20. Kim, Y. M., Yun, J., Lee, C. K., Lee, H., Min, K. R., & Kim, Y. (2002) Oxyresveratrol and hydroxystilbene compounds. Inhibitory effect on tyrosinase and mechanism of action. *Journal of Biological Chemistry, 277*, 16340–16344.
21. Dowd, P. F. (1999) Relative inhibition of insect phenoloxidase by cyclic fungal metabolites from insect and plant pathogens. *Natural Toxins, 7*, 337–341.
22. Kubo, I., Kinst-Hori, I., Nihei, K., Soria, F., Takasaki, M., Calderón, J. S., et al. (2003) Tyrosinase inhibitors from galls of *Rhus javanica* leaves and their effects on insects. *Zeitschrift für Naturforschung. C, A Journal of Biosciences, 58c*, 719–725.
23. Wang, S. D., Luo, W. C., Xu, S. J., & Ding, Q. (2005) Inhibitory effects of 4-dodecylresrcinol on the phenoloxidase of the diamondback moth *Plutella xylostella* (*L.*) (*Lepidoptera: plutellidae*). *Pesticide Biochemistry and Physiology, 82*, 52–58.
24. Chen, Q. X., Ke, L. N., Song, K.K., Huang, H., & Liu, X. D. (2004) Inhibitory effects of hexylresorcinol and dodecylresorcinol on mushroom (*Agaricus bisporus*) tyrosinase. *Protein Journal, 23*, 135–141.
25. Qiu, L., Chen, Q. X., Wang, Q., Huang, H., & Song, K. K. (2005) Irreversibly inhibitory kinetics of 3,5-dihydroxyphenyl decanoate on mushroom (*Agaricus bisporus*) tyrosinase. *Bioorganic and Medicinal Chemistry, 13*, 6206–6211.
26. Chen, Q. X., Song, K.K., Qiu, L., Liu, X. D., Huang, H., & Guo, H. Y. (2005) Inhibitory effects on mushroom tyrosinase by *p*-alkoxybenzoic acids. *Food Chemistry, 91*, 269–274.
27. Song, K. K., Huang, H., Han, P., Zhang, C. L., Shi, Y., & Chen, Q. X. (2006) Inhibitory effects of cis- and trans-isomers of 3,5-dihydroxystilbene on the activity of mushroom tyrosinase. *Biochemical and Biophysical Research Communications, 342*, 1147–1151.
28. Xie, X. Y., Jiang, L., Xue, C. B., & Luo, W. C. (2007) Synthesis of substituted benzaldehyde thiosemicarbazones and its activity for inhibition of the phenoloxidase of the diamondback moth *Plutella xylostella* (*L.*). *Chemical Reagents, 29*, 34–36. (in Chinese).
29. Jiménez, M., Chazarra, S., Escribano, J., Cabanes, J., & Garcia-Carmína, F. (2001) Competitive inhibition of mushroom tyrosinase by 4-substituted benzaldehydes. *Journal of Agricultural and Food Chemistry, 49*, 4060–4063.
30. Chen, Q. X., & Kubo, I. (2002) Kinetics of mushroom tyrosinase inhibition by quercetin. *Journal of Agricultural and Food Chemistry, 50*, 4108–4112.
31. Espín, J. C., & Wichers, H. J. (1999) Slow-binding inhibition of mushroom (*Agaricus bisporus*) tyrosinase isoforms by tropolone. *Journal of Agricultural and Food Chemistry, 47*, 2638–2644.
32. Tsou, C. L. (1988) Kinetics of substrate reaction during irreversible modification of enzyme activity. *Advances in Enzymology and Related Areas in Molecular Biology, 61*, 381–436.